

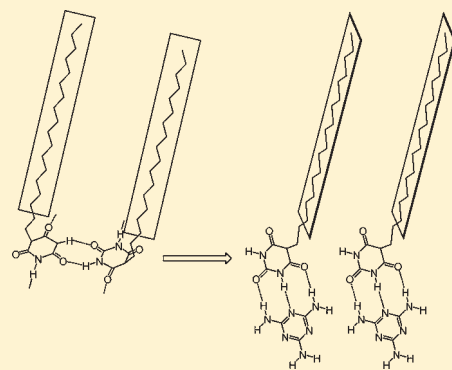
In Situ IRRAS Studies of Molecular Recognition of Barbituric Acid Lipids to Melamine at the Air–Water Interface

Xianming Kong and Xuezhong Du*

Key Laboratory of Mesoscopic Chemistry (Ministry of Education), State Key Laboratory of Coordination Chemistry, and School of Chemistry and Chemical Engineering, Nanjing University, Nanjing 210093, People's Republic of China

S Supporting Information

ABSTRACT: Recognition and detection of melamine are of very significance in food industries. Molecular recognitions of barbituric acid lipids to melamine at the air–water interface have been investigated in detail using in situ infrared reflection absorption spectroscopy (IRRAS). Hydrogen bonding patterns and molecular orientations of the molecular recognitions have been revealed. Prior to molecular recognition, the barbituric acid moieties in the monolayers were hydrogen bonded with a flat-on fashion at the air–water interface, and the alkyl chains were preferentially oriented with their CCC planes perpendicular to the water surface. After molecular recognition, the NH_2 stretching bands of recognized melamine were clearly observed at the air–water interface as well as primary characteristic bands, the barbituric acid moieties underwent a change in orientation with non-hydrogen bonded $\text{C}4=\text{O}$ bonds almost perpendicular to the water surface and $\text{C}2=\text{O}$ and $\text{C}6=\text{O}$ bonds involved in hydrogen bonds with melamine, and the alkyl chains were preferentially oriented with their CCC planes parallel to the water surface. The monolayers of barbituric acid lipids exhibited excellent selectivity for melamine over nucleosides.



INTRODUCTION

Since 2008, melamine has attracted much attention in the scandal of illegally adding melamine to dairy products to falsely increase protein content. This has led to serious kidney damages in tens of thousands of infants and even several cases of death.^{1,2} The damaging effect is considered to likely result from the aggregates of melamine with associated impurities or metabolites existing in body fluids such as cyanuric acid and uric acid bearing imide moieties.^{3,4} It is obvious that recognition and detection of melamine become more important than ever. Molecular recognition is one of the most important processes for the construction of biological assemblies. The mutual recognition of complementary components by means of multiple hydrogen bonds is not only a vital biological process⁵ but also the basis for the construction of a variety of sensors. However, the hydrogen bonding interactions cannot yield significant driving forces for molecular recognition in bulk water due to the strong competitive binding of water molecules.⁶ Langmuir monolayers at the air–water interface, with half a framework structure of cellular membranes, provide unique microenvironments for molecular interactions⁷ and have been developed in the past decades to mimic molecular recognition.^{8–10} The molecular recognitions of barbituric acid and melamine derivatives at the air–water interface and in Langmuir–Blodgett (LB) films have been extensively studied,^{11–20} but most of the works are limited to the recognitions of melamine-derived lipids to barbituric acid in aqueous subphase^{14–20} because characteristic infrared peaks of barbituric acid ($\text{C}=\text{O}$ stretching vibration) can be readily detected from transferred LB films. However, the information on molecular

orientation and structure of the LB films is not equivalent to that obtained directly from the monolayers at the air–water interface.

Infrared reflection absorption spectroscopy (IRRAS) has been a leading structural method for the in situ characterization of the monolayers at the air–water interface on the molecular level.^{21–31} Weck et al.¹³ used the IRRAS technique in 1997 to study the hydrogen bonding interactions between barbituric acid lipid monolayers and melamine from aqueous subphase. However, in general, the quality of these spectra is not ideal.¹⁷ Huo et al.¹⁷ used polarization modulated–IRRAS (PM–IRRAS) technique in 1999 to study the hydrogen bonding interactions between melamine-derived lipid monolayers and barbituric acid. So far, few studies have been devoted to the molecular recognitions by means of hydrogen bonds at the air–water interface using the IRRAS technique.^{13,17,32,33}

In this paper, molecular recognitions between the monolayers of barbituric acid lipids at the air–water interface and melamine in aqueous subphases have been investigated in detail along with the selectivity of molecular recognitions in the presence of other molecules (such as nucleosides) with complementary donating and accepting groups for probable hydrogen bonding interactions with the barbituric acid moieties, the chemical structures of which are presented in Figure 1. Some new information on hydrogen bonding patterns and molecular orientations of the molecular recognitions has been obtained.

Received: August 16, 2011

Revised: October 2, 2011

Published: October 13, 2011

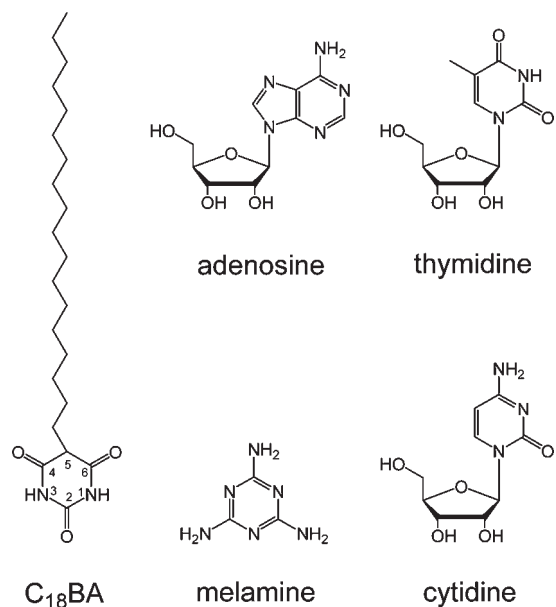


Figure 1. Chemical structures of 5-octadecylbarbituric acid (C₁₈BA), melamine, adenosine, thymidine, and cytidine.

EXPERIMENTAL SECTION

Chemicals. The chemical reagents used in the experiments were commercially available. 1-Bromooctadecane (98%), diethyl malonate (99%), urea (99%), sodium (99.7%), melamine (99%), and ethanol (99%) were purchased from Sinopharm Chemical Reagent Co., Ltd. Adenosine (97%), thymidine (99%), and cytidine (99%) were acquired from Fluka. Ethanol was purified to exclude water by the standard procedures³⁴ prior to use, and other chemical reagents were used as received. 5-Octadecylbarbituric acid (C₁₈BA) was synthesized according to the method reported previously¹³ with a small modification in amount of reactants and volume of solvents. The water used was double distilled (pH 5.6, resistivity of 18.2 MΩ cm, surface tension of 73.06 mN/m at 22 °C) after a deionized exchange.

Preparation of Diethyl β-Octadecylmalonate. Diethyl malonate of 1.60 g (10 mmol) was dissolved in 10 mL of absolute ethanol containing 0.23 g (10 mmol) of sodium. The mixture was heated to reflux for 20 min, and then 3.33 g of 1-bromooctadecane (10 mmol) was added dropwise within 2 min. The reflux continued for 3 h under ambient conditions, and the mixture was then filtered before cooling. The filtrate was concentrated to yield colorless oil, and the crude product was further purified by column chromatography (silica gel, ethyl acetate/hexane, 1:20, v/v) to give diethyl β-octadecylmalonate of colorless oil. ¹H NMR (500 MHz, CDCl₃): δ 4.21 (q, 4H, 2OCH₂), 3.33 (t, 1H, CH), 1.90 (q, 2H, CH₂), 1.30 (m, 38H, 16CH₂ + 2CH₃), 0.90 (t, 3H, CH₃).

Synthesis of C₁₈BA. A total of 0.24 g of urea (4 mmol) was dissolved in 10 mL of absolute ethanol containing 0.28 g (12 mmol) of sodium. The mixture was heated to reflux for 20 min, and then 1.56 g of diethyl β-octadecylmalonate (3.8 mmol) was added dropwise within 2 min. The reflux continued for 9 h under ambient conditions, so that most of the solvent was evaporated out. Then 40 mL of water was added to the residue, and the pH was adjusted to 5.0–6.0 with hydrochloric acid. The precipitate was isolated by suction filtration and washed with water.

The crude product was further purified by recrystallization from ethanol for three times to yield white crystal. ¹H NMR (500 MHz, DMSO): δ 11.20 (s, 2H, 2NH); 3.51 (t, 1H, CH), 1.87 (q, 2H, CH₂), 1.26 (m, 32H, 16CH₂), 0.86 (t, 3H, CH₃). ESI-MS *m/z*: calcd for C₂₂H₄₀N₂O₃, 380.5; found 379.5 (M–H)[–].

Monolayer Isotherms and LB Film Preparation. The spreading and transfer of the monolayers were performed on a Nima 611 Langmuir trough with two barriers. A Wilhelmy plate (a piece of filter paper) was used as the surface pressure sensor and situated in the middle of the trough. Monolayers were obtained by spreading the chloroform solution of C₁₈BA on aqueous subphases. The subphase temperature was kept at 22 °C. For the preparation of LB films, the monolayers were first compressed to a desired surface pressure of 20 mN/m, and then 30 min was allowed for the monolayers to reach equilibrium. For CaF₂ substrates, 3-layer LB films (Y type) were transferred on two sides by the vertical method at a dipping rate of 2.0 mm/min with the transfer ratios of nearly unity for upstroke and about 0.8 for downstroke. For gold-coated silicon wafers, first monolayer was deposited by the vertical method with a transfer ratio of nearly unity, and following 20 layers (Y type) were transferred on one side by the horizontal method at a dipping rate of 2.0 mm/min with a transfer ratio of about 2.

IRRAS Spectrum Measurements. IRRAS spectra of the monolayers at the air–water interface were recorded on an Equinox 55 FTIR spectrometer (Bruker) connected to an XA-511 external reflection attachment with a shuttle trough system and a liquid-nitrogen-cooled MCT detector. Sample (monolayer-covered surface) and reference (monolayer-free surface) troughs were fixed on a shuttle device driven by a computer-controlled stepper motor for allowing collection from the two troughs in an alternate mode at 22 °C. A KRS-5 polarizer was used to generate p- and s-polarized lights. The C₁₈BA molecules were spread from their chloroform solution, and 20 min was allowed for solvent evaporation. The measurement system was then enclosed for humidity equilibrium and monolayer relaxation for 4 h prior to compression. The external reflection absorption spectra of aqueous solutions were used as references, respectively. The monolayers were compressed discontinuously to the desired surface pressure of 20 mN/m from approximately 0 mN/m. After 30 min of relaxation, the two moving barriers were stopped and the monolayer areas were kept constant. The spectra at different surface pressures were collected at an incidence angle of 30°, and the spectra at 20 mN/m with the incidence angles from 30° to 65° to obtain information on molecular orientation. The spectra were recorded with a resolution of 8 cm^{–1} by coaddition of 1024 scans. A time delay of 30 s was allowed for film equilibrium between trough movement and data collection. Spectra were acquired using p-polarized radiation followed by data collection using s-polarized one. The IRRAS spectra were used without smoothing or baseline correction.

FTIR Spectrum Measurements. FTIR transmission (TR) spectra of the LB films on CaF₂ substrates were recorded on a VERTEX 70 V spectrometer (Bruker) with a DTGS detector. Typically 1024 scans were collected to obtain a satisfactory signal-to-noise ratio with the resolution 4 cm^{–1}. The film spectra were obtained by subtracting the spectra of blank CaF₂ substrates from the corresponding sample spectra. Reflection absorption (RA) spectra of the LB films on gold-coated silicon wafers were recorded on the FTIR spectrometer at an incidence angle of 80° with a bare gold-coated wafer as a reference. The spectra were recorded with a resolution of 4 cm^{–1} by coaddition of 1024 scans.

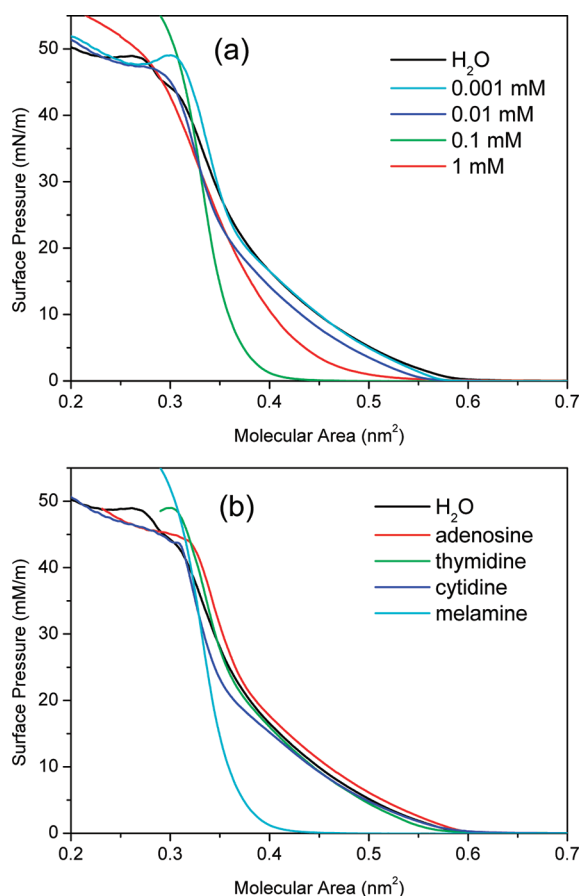


Figure 2. Surface pressure–area isotherms of the monolayers of $C_{18}BA$ at the air–water interface: (a) on aqueous melamine subphases with different concentrations and (b) on aqueous subphases containing nucleosides (0.1 mM).

RESULTS AND DISCUSSION

Isotherms of Monolayers at the Air–Water Interface.

Surface pressure–area (π – A) isotherms of the monolayers of $C_{18}BA$ on pure water and aqueous melamine subphases are shown in Figure 2a. $C_{18}BA$ lipids formed a stable monolayer with a transition from the limiting area of 0.515 to 0.416 nm² and a collapse pressure of about 45 mN/m. The limiting area was much greater than the cross-sectional area of hydrocarbon chains (ca. 0.20 nm²), which indicates that the limiting area of the lipids was predominantly determined by barbituric acid moieties. The crystal structure of barbituric acid dihydrate, which is selected for consideration since the lipids were spread at the air–water interface, is determined to be orthorhombic with the unit cell dimensions $a = 1.274$, $b = 0.624$, and $c = 0.889$ nm containing four molecules.³⁵ The crystal structure consists of planar layers of barbituric acid and water molecules hydrogen-bonded into a compact arrangement.³⁵ On the basis of the dimensions,³⁵ each barbituric acid dihydrate occupied an area of 0.566 nm² when lying flat on a plane. It was obvious that the barbituric acid moieties initially almost adopted a flat-on orientation on the water surface. This suggested the formation of intermolecular hydrogen bonds between adjacent barbituric acid moieties and between barbituric acid and water molecules. In the presence of melamine in the aqueous subphases, the isotherm underwent a change dependent on melamine concentration.

Melamine of low concentrations (0.001 mM) hardly caused a change in isotherm, and a slight condensation of the isotherm was observed upon increase of melamine concentration to 0.01 mM. In the case of 0.1 mM melamine, the isotherm was considerably condensed with a limiting area of 0.363 nm²; however, an increase in limiting area was followed upon further increase of melamine concentration to 1 mM. This means that molecular recognitions between the barbituric acid moieties and melamine occurred at the relatively high concentrations of melamine, concomitant with a change in orientation of barbituric acid planes from a flat-on fashion to an end-on one followed by a rotation of C_{2v} symmetry axis of the planes. In the presence of adenosine, thymidine, and cytidine (0.1 mM) individually in the aqueous subphases, only a slight change in isotherm occurred in the cases of adenosine and cytidine, and no change was observed in the case of thymidine because of the similar chemical structure to barbituric acid (Figure 2b).

IRRAS Spectra of Monolayers at the Air–Water Interface.

It is well-known that IRRAS data are defined as plots of reflectance–absorbance versus wavenumber. Reflectance–absorbance is defined as $-\log(R/R_0)$, where R and R_0 are the reflectivities of the monolayer-covered and monolayer-free surfaces, respectively. The “metal selection rule” does not apply to the air–water interface, because water is a low absorbing substrate and the intensity of the reflected beam is much lower than the intensity of the incoming beam. Therefore, all of three electric field components have a sufficiently high intensity at the water surface to interact with the monolayers. In the case of s-polarization, the electric field vector is perpendicular to the plane of incidence, i.e., parallel to the water surface. The bands are always negative and their intensities decrease with increasing incidence angle.^{21,25,27} In the case of p-polarization, the electric field vector is parallel to the plane of incidence: (i) for the vibrational transition moments parallel to the water surface, the bands are initially negative and their intensities increase with increasing incidence angle and reach maximum values, then minima in the reflectivity occur at the Brewster angle, and above the Brewster angle the bands become positive and their intensities decrease upon further increase of incidence angle;^{21,25,27} (ii) for the vibrational transition moments perpendicular to the water surface, the bands are first positive and then become negative above the Brewster angle;^{21,27,28,36,37} (iii) if the vibrational transition moments are tilted to the air–water interface, the intensities of the bands are weak and even zero.³⁶

Figure 3 shows p-polarized IRRAS spectra of the monolayers of $C_{18}BA$ on pure water at various surface pressures. These spectral behaviors were very similar except for band intensities, and their band frequencies were almost independent of surface pressure. The spectral baselines were distorted in the regions corresponding to the vibrational transitions of water because of the altered structure of the water adjacent to the headgroups of the film constituents, and the distortions were maximal for small incidence angles. The two bands at 2919 and 2852 cm^{−1} were assigned to the antisymmetric and symmetric CH_2 stretching vibrations [$\nu_a(CH_2)$ and $\nu_s(CH_2)$] of alkyl chains,^{38,39} respectively. It is well-known that the $\nu_a(CH_2)$ and $\nu_s(CH_2)$ frequencies are sensitive to conformation order of alkyl chains.^{38,39} Lower wavenumbers are characteristic of all-trans conformations in highly ordered chains, while higher wavenumbers are indicative of gauche conformations in highly disordered chains.^{38,39} It is clear that the alkyl chains in these monolayers were basically ordered but with a small amount of gauche conformers. It is

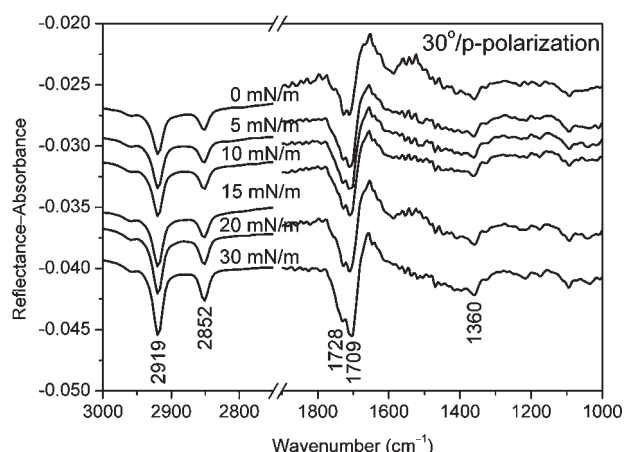


Figure 3. p-Polarized IRRAS spectra of the monolayers of $C_{18}BA$ at the air–water interface on pure water at different surface pressures at an incidence angle of 30° .

noted that the $\nu_a(CH_2)$ band intensities were nearly twice higher than the $\nu_s(CH_2)$ ones at various surface pressures, which indicates that the alkyl chains were preferentially oriented with their CCC planes perpendicular to the water surface. The strong doublet bands at 1728 and 1709 cm^{-1} were attributed to the C=O stretching vibrations of the barbituric acid moieties.⁴⁰ The frequency of the C=O stretching band is strongly dependent on hydrogen bonding. The C=O stretching band of barbituric acid in an argon matrix appears at 1754 cm^{-1} for the monomer and 1732 cm^{-1} for the dimer.⁴⁰ These peaks shift to 1694 cm^{-1} in the solid state at 20 K, owing to hydrogen bonding formation between barbituric acid molecules.⁴⁰ The formation of the hydrogen bonds weakens C=O bond strength, and the C=O stretch occurs at lower vibrational frequency. It is clear that the intermolecular hydrogen bonds were formed between the adjacent barbituric acid moieties in the monolayers, so that the planes of barbituric acid preferentially adopted a flat-on orientation on the water surface.

Figure 4a shows p-polarized IRRAS spectra of the monolayers of $C_{18}BA$ on aqueous melamine subphases with different concentrations at the surface pressure of 20 mN/m at an incidence angle of 30° . On the aqueous melamine subphase of 0.01 mM, no significant spectral change was detected except for a weak negative peak at 1762 cm^{-1} , but remarked spectral features were observed upon increase of melamine concentration to 0.1 and 1 mM. These new peaks at 3354 (NH_2 antisymmetric stretching), 3242 (NH_2 symmetric stretching), 1632 (NH_2 scissoring), 1539 (quadrant triazine ring stretching),¹⁷ 1452 (semicircle ring stretching),¹⁷ and 1425 cm^{-1} (semicircle ring stretching)¹⁷ resulted from melamine due to the occurrence of molecular recognition between the barbituric acid moieties and melamine. The assignments of the bands for the monolayers are listed in Table 1. We first reported in situ IRRAS detection of NH stretching vibrational bands from the monolayers at the air–water interface,⁴² and those NH stretching bands resulted from amide groups of the host monolayers.^{42–44} Herein, the detected NH_2 stretching bands were attributed to the vibrational transitions of amino groups of recognized melamine molecules. NH stretching bands from amino groups at the air–water interface have not been observed using the IRRAS technique before. A strong C=O stretching band from barbituric acid shifted down to 1691 cm^{-1} , indicating the occurrence of molecular recognition,

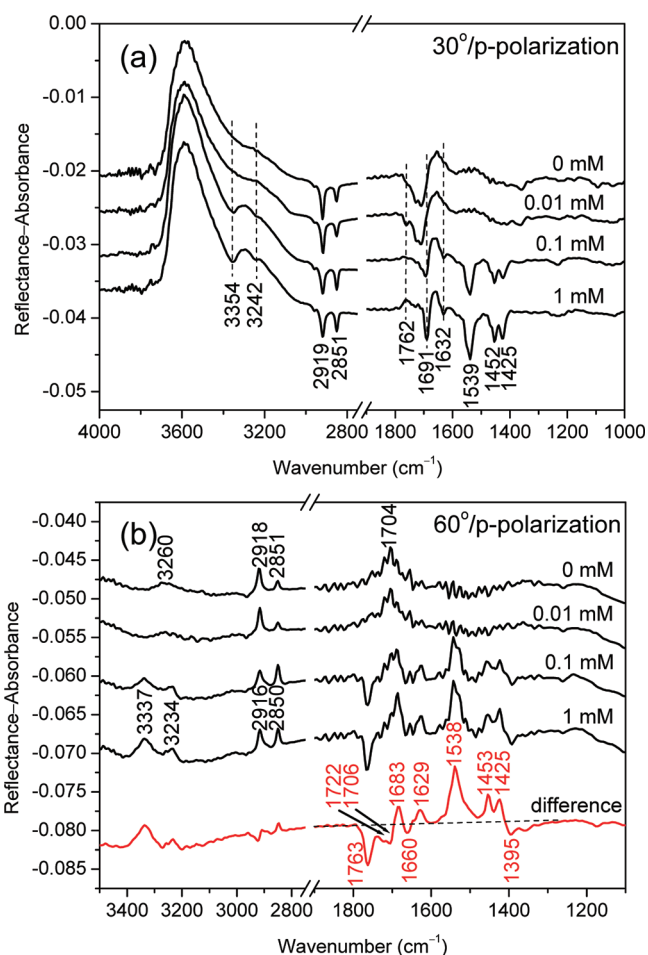


Figure 4. p-Polarized IRRAS spectra of the monolayers of $C_{18}BA$ at the air–water interface on aqueous melamine subphases with various concentrations at 20 mM/m at different incidence angles: (a) 30° and (b) 60° , together with a difference spectrum in the presence and absence of 1 mM melamine.

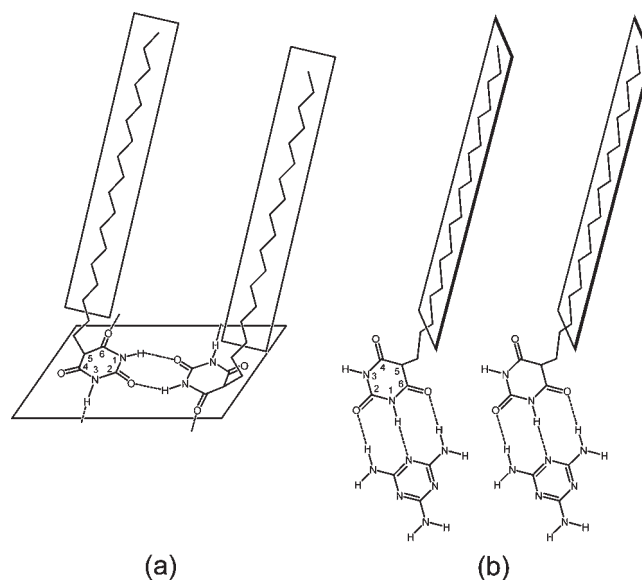
meanwhile, a positive peak at 1762 cm^{-1} appeared at the incidence angle of 30° in the case of 1 mM melamine, and a strong negative band at 1763 cm^{-1} was clearly observed at the incidence angle of 60° (above the Brewster angle, Figure 4b), which indicates that non-hydrogen bonded C=O groups appeared, with their vibrational transition moments almost perpendicular to the water surface. For the monolayers of *N*-substituted barbituric acid lipids on aqueous melamine subphases, Weck et al.¹³ also observed the shifts to high wavenumbers (although the quality of the spectra is not ideal) but could not give a clear explanation. In the alternate LB films of $C_{18}BA$ and *N,N*-substituted melamine lipids, free C=O stretching bands at 1755 cm^{-1} were observed at the high surface pressures of 15 and 20 mN/m.¹⁸ The free C=O groups were considered not to interact with any group in the tilted molecule model.¹⁸ From Figure 4b, an obvious negative band was also observed in the case of 0.1 mM melamine but was weaker in intensity than that in the case of 1 mM melamine. Considering the smaller molecular area and higher molecular density in the case of 0.1 mM melamine (Figure 2a), the free C=O (either C4=O or C6=O) bonds of barbituric acid moieties in the monolayers in the case of 1 mM melamine were more perpendicular to the water surface than those in the case of 0.1 mM melamine.

Table 1. Absorption Bands and Their Assignments of IRRAS Spectra of the C₁₈BA Monolayers on Different Aqueous Subphases and Transmission and Reflection Absorption Spectra of the Corresponding LB Films

| wavenumber (cm ⁻¹) ^a | | | | | | | | | |
|---|------------------------|-----------|-----------|------------------|--------|------------------|--------|--------------------------|--|
| IRRAS/monolayers | | | | TR/LB films | | RA/LB films | | orientation ^b | assignment ^c |
| H ₂ O (30°) | H ₂ O (60°) | mel (30°) | mel (60°) | H ₂ O | mel | H ₂ O | mel | | |
| | | 3354 w | 3337 m | | 3341 m | | | | $\nu_{\text{a}}(\text{NH}_2)^{18}$ |
| | 3260 w | | | 3238 w | | | | | $\nu(\text{NH})^{40}$ |
| | | 3242 w | 3234 m | | 3234 w | | | | $\nu_{\text{s}}(\text{NH}_2)$ |
| | | | | 3089 w | | | | | $\nu(\text{NH})^{40}$ |
| 2959 | | 2958 | | 2956 | 2956 | 2956 | 2960 | | $\nu_{\text{a}}(\text{CH}_3)$ |
| 2919 s | 2918 m | 2919 s | 2916 m | 2918 s | 2918 s | 2919 s | 2920 s | | $\nu_{\text{a}}(\text{CH}_2)^{38,39}$ |
| 2852 m | 2851 w | 2851 s | 2850 m | 2850 m | 2851 s | 2851 s | 2851 m | | $\nu_{\text{s}}(\text{CH}_2)^{38,39}$ |
| | | 1762 w | 1763 s | | 1760 w | | 1762 s | ⊥ | $\nu(\text{C=O})^{18,40}$ |
| 1728 s | | 1691 s | 1683 m | 1735 m | | 1739 s | | | $\nu(\text{C=O})^{18,40}$ |
| 1709 s | 1704 | | | 1692 m | 1687 s | 1691 w | | | $\nu(\text{C=O})^{40}$ |
| | | | 1660 w | 1675 m | | 1674 w | 1666 m | ⊥ | $\nu(\text{C=O})^{40}$ |
| | | 1632 w | 1629 w | | 1626 m | | | | $\delta(\text{NH}_2)^{17}$ |
| | | | | | | | 1580 w | | $\nu(\text{Q ring})^{17}$ |
| | | | | | | | 1557 m | | $\nu(\text{Q ring})^{17}$ |
| | | 1539 s | 1538 s | | 1540 s | | 1538 w | | $\nu(\text{Q ring})^{17}$ |
| | | | | 1470 w | 1468 w | 1471 m | 1468 w | | $\delta(\text{CH}_2)^{41} + \nu(\text{S ring})^{17}$ |
| | | 1452 s | 1453 m | | 1442 m | 1430 w | | | $\nu(\text{S ring})^{17}$ |
| | | 1425 s | 1425 m | | 1424 m | | | | $\nu(\text{S ring})^{17}$ |
| | | | 1395 w | | | | 1396 m | ⊥ | $\nu(\text{S ring})^{17}$ |
| 1360 w | | | 1359 w | 1358 w | | 1358 w | | | $\nu(\text{S ring})^{17}$ |

^a s, strong; m, medium; w, weak. ^b ||, parallel to substrate; ⊥, perpendicular to substrate. ^c ν , stretching; ν_a , antisymmetric stretching; ν_s , symmetric stretching; δ , bending; Q, quadrant; S, semicircle.

That means that the C_{2v} symmetry axis of barbituric acid planes was tilted away from the normal of the monolayer and a relatively big room was required for the C5-substituted alkyl chains to orient upward in the case of 1 mM melamine, leading to an increase in molecular area. The IRRAS data well supported the behaviors of corresponding isotherms dependent on melamine concentration. The $\nu_s(\text{CH}_2)$ band intensities were considerably increased after molecular recognition, even larger than the $\nu_a(\text{CH}_2)$ ones in the case of 0.1 mM melamine at the incidence angle of 60° (Figure 4b), which indicates that the CCC planes of the alkyl chains were preferentially oriented parallel to the water surface. From the p- and s-polarized IRRAS spectra at different incidence angles before and after molecular recognition (Figures S1–S3 in the Supporting Information), the $\nu_a(\text{CH}_2)/\nu_s(\text{CH}_2)$ intensity ratio as a function of incidence angle (Figure S4) further demonstrates that the alkyl chains underwent a change with their CCC planes from perpendicular to the water surface²⁹ before molecular recognition to parallel to the water surface²⁸ after molecular recognition. The illustration of the molecular recognition between the monolayers of barbituric acid lipids and melamine was schematically represented in Figure 5 (C4=O bonds are drawn to be non-hydrogen-bonded). Owing to the inherent weak signals and interference of water vapor at the incidence angle of 60°, a difference spectrum in the presence and absence of 1 mM melamine was presented in Figure 4b for comparison. A negative dip at 1660 cm⁻¹ appeared in the difference spectrum. It is not unambiguous to determine whether it was a vibrational band (C=O stretching vibration of barbituric acid or NH₂ scissoring one of melamine) or a false peak. In the

**Figure 5.** Schematic illustration of hydrogen bonding patterns and molecular orientations of barbituric acid lipids and melamine at the air–water interface before and after molecular recognition.

following, a band at 1666 cm⁻¹ was obviously observed in the RA spectrum of the corresponding LB film (Figure 6), which indicates that the above “negative dip” was a vibrational band. In the solid state of hydrogen bonded melamine, the NH₂

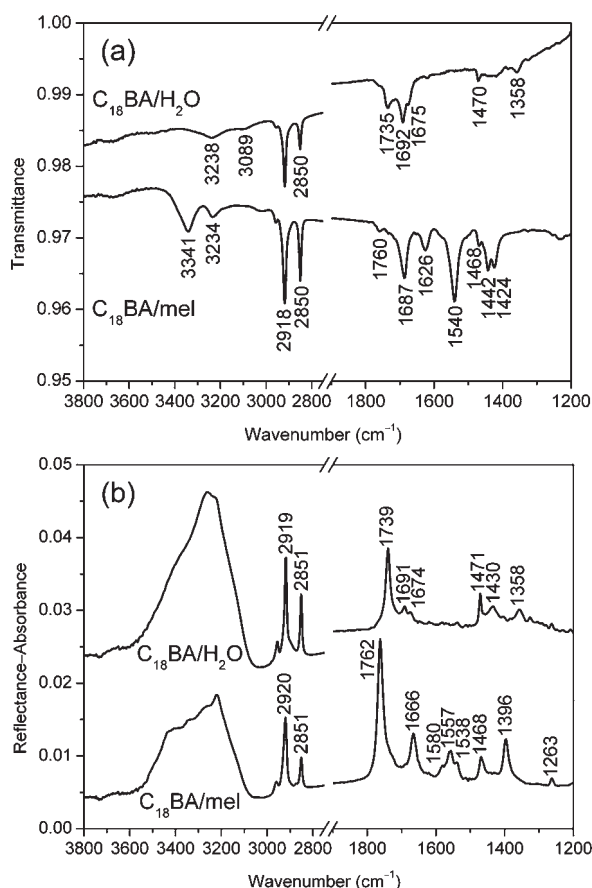


Figure 6. FTIR spectra of the LB films of $C_{18}BA$ transferred from pure water and aqueous melamine subphase (0.1 mM): (a) transmission (TR) mode and (b) reflection absorption (RA) mode.

scissoring band appeared at 1653 cm^{-1} ;¹⁷ however, the band appeared at 1627 cm^{-1} in aqueous melamine solution (Figure S5). At the air–water interface, the NH_2 scissoring band of melamine shifted up to 1632 cm^{-1} (Figure 4a) due to the occurrence of the molecular recognition between barbituric acid moieties and melamine. It is known that when hydrogen bonds are formed the stretching vibrations occur with lower frequencies and the scissoring ones with higher frequencies. It is clear that the peak at 1660 cm^{-1} in the difference spectrum resulted from the downshift of the $C=O$ stretching band after molecular recognition, which was attributed to $C2=O$ bonds of the barbituric acid moieties with the vibrational transition moments perpendicular to the water surface to a great extent.

FTIR Spectra of LB Films. In order to give a deep insight into the molecular structures of the monolayers before and after molecular recognition, the corresponding LB films were studied using a combination of TR and RA modes of FTIR spectroscopy (Figure 6), and the assignments of the absorption bands are also listed in Table 1. The absorption bands are very strong in the TR spectra when their transition moments are parallel to the substrate surface, and the bands are very strong in the RA spectra when their transition moments are perpendicular to the substrate surface. For the LB film of barbituric acid lipids from pure water, both $\nu_a(CH_2)$ and $\nu_s(CH_2)$ bands in the TR and RA modes were obviously observed, which indicates that the alkyl chains were tilted away from the surface normal, moreover the $\nu_a(CH_2)/\nu_s(CH_2)$ intensity ratio in the TR mode was much larger than

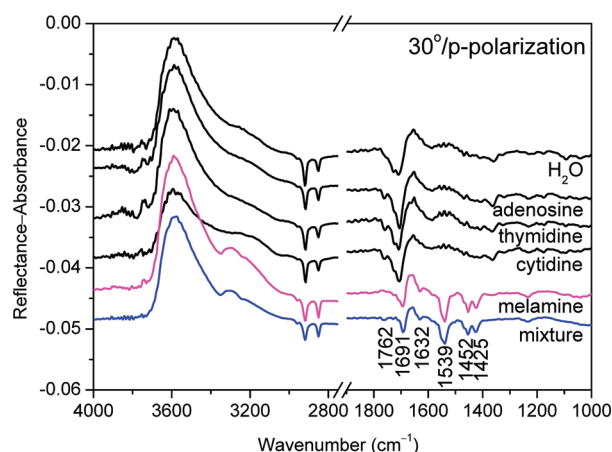


Figure 7. p-Polarized IRRAS spectra of the monolayers of $C_{18}BA$ at the air–water interface on different aqueous subphases (0.1 mM, the mixture containing thymidine, cytidine, and melamine) at 20 mM/m at an incidence angle of 30° .

that in the RA mode, which suggests that the CCC planes of the alkyl chains were preferentially oriented perpendicular to the substrate surface. The $C=O$ stretching bands at 1735 , 1692 , and 1675 cm^{-1} in the TR mode corresponded to the those at 1739 , 1691 , and 1674 cm^{-1} in the RA mode. For the LB film from aqueous melamine subphase, both $\nu_a(CH_2)$ and $\nu_s(CH_2)$ bands in the TR and RA modes were also clearly observed, but the $\nu_a(CH_2)/\nu_s(CH_2)$ intensity ratio in the TR mode was smaller than that in the RA mode, which suggests that the CCC planes of the alkyl chains were preferentially oriented parallel to the substrate surface. After molecular recognition, a weak free $\nu(C=O)$ band at 1760 cm^{-1} in the TR mode corresponded to a strong band at 1762 cm^{-1} in the RA mode, which indicates that the $C4=O$ bonds were oriented nearly perpendicular to the substrate surface. A band at 1666 cm^{-1} in the RA mode was clearly observed, which was the downshift of the $\nu(C=O)$ band at 1674 cm^{-1} before molecular recognition. This spectral feature indicates that the weak $C2=O$ bonds underwent a change in orientation after molecular recognition. Meanwhile, a new band at 1396 cm^{-1} due to the semicircle ring stretch of melamine¹⁷ in the RA mode was obviously observed. Compared with Figure 6b, the negative dip at 1660 cm^{-1} in the difference spectrum of Figure 4b was owing to the $C2=O$ stretching vibration with the transition moment almost perpendicular to the water surface. The observed bands at 1540 , 1442 , and 1424 cm^{-1} in the TR mode and the bands at 1580 , 1557 , 1538 , and 1396 cm^{-1} in the RA mode were attributed to the quadrant and semicircle ring stretches of melamine¹⁷ with most of their transition moments perpendicular to each other.

Selectivity of Molecular Recognition. Figure 7 compares p-polarized IRRAS spectra of the monolayers of $C_{18}BA$ on pure water and aqueous subphases containing adenosine, thymidine, cytidine, melamine, and their mixtures at 20 mM/m at the incidence angle of 30° , respectively. The monolayers on the aqueous subphases containing nucleosides individually exhibited slight spectral changes in comparison with that on pure water. A negative peak at 1762 cm^{-1} was observed in these cases in contrast to a positive peak in the case of melamine. The most characteristic absorption bands of the nucleosides should be apparent in the vicinity of 1700 and/or 1650 cm^{-1} , which made it difficult to distinguish these characteristic bands because of the

absorption bands of the barbituric acid moieties and distorted spectral baselines. However, no characteristic band of cytidine ($1600\text{--}1620\text{ cm}^{-1}$)^{32,33} was clearly observed, which indicates that cytidine did not efficiently bind to the C₁₈BA monolayer. Combining with the spectra at the incidence angle of 60° (Figure S6), the nucleosides with complementary donating/accepting groups could not be effectively recognized in the monolayers of C₁₈BA. On the aqueous subphase containing the mixture of thymidine, cytidine, and melamine, the monolayer almost displayed the same spectrum as that in the presence of melamine only. The barbituric acid moieties exhibited excellent selectivity for melamine over nucleosides. The same conclusion is also obtained from the FTIR spectra of the corresponding LB films (Figure S7). From their chemical structures, double hydrogen bonds could be only formed between the nucleosides and barbituric acid against the double hydrogen bonds between the barbituric acid moieties, whereas triple hydrogen bonds could be readily formed between melamine and barbituric acid.

CONCLUSIONS

Melamine binding to the monolayers of barbituric acid lipids at the air–water interface has been investigated in detail using the IRRAS technique, together with the FTIR studies of the corresponding LB films. On pure water, the barbituric acid moieties in the monolayer were hydrogen bonded with their planes to take a flat-on mode, and the CCC planes of the alkyl chains were preferentially oriented perpendicular to the water surface. After molecular recognition, the NH₂ stretching bands from the amino groups of recognized melamine were clearly detected at the air–water interface as well as primary characteristic bands. NH stretching bands from amino groups at the air–water interface have not been observed using the IRRAS technique before. The barbituric acid moieties underwent a change in orientation with non-hydrogen bonded C4=O bonds almost perpendicular to the water surface and other hydrogen bonded C=O bonds (C2=O bonds perpendicular to the water surface to a great extent and C6=O ones almost parallel to), and the CCC planes of the alkyl chains were preferentially oriented parallel to the water surface. The monolayers of barbituric acid lipids exhibited excellent selectivity for melamine over nucleosides.

ASSOCIATED CONTENT

S Supporting Information. IRRAS spectra (p- and s-polarization) of the C₁₈BA monolayers on pure water and aqueous melamine subphases at the surface pressure of 20 mN/m against different incidence angles, the $\nu_a(\text{CH}_2)/\nu_s(\text{CH}_2)$ intensity ratio as a function of incidence angle, FTIR spectra of melamine in powder and in aqueous solution, p-polarized IRRAS spectra of the C₁₈BA monolayers on pure water and aqueous subphases containing adenosine, thymidine, cytidine, melamine, and their mixtures at 20 mM/m at the incidence angle of 60°, and FTIR spectra of the corresponding LB films. This material is available free of charge via the Internet at <http://pubs.acs.org>.

AUTHOR INFORMATION

Corresponding Author

*E-mail: xzdu@nju.edu.cn. Fax: 86-25-83317761.

ACKNOWLEDGMENT

This work was supported by the National Natural Science Foundation of China (No. 20873062) and the Fundamental Research Funds for the Central Universities (1103020503).

REFERENCES

- (1) Chan, E. Y. Y.; Griffiths, S. M.; Chan, C. W. *Lancet* **2008**, 372, 1444–1445.
- (2) Shen, J.-S.; Cai, Q.-G.; Jiang, Y.-B.; Zhang, H.-W. *Chem. Commun.* **2010**, 46, 6787–6788.
- (3) Hau, A. K.-c.; Kwan, T. H.; Li, P. K.-t. *J. Am. Soc. Nephrol.* **2009**, 20, 245–250.
- (4) Dobson, R. L. M.; Motlagh, S.; Quijano, M.; Cambron, R. T.; Baker, T. R.; Pullen, A. M.; Regg, B. T.; Bigalow-Kern, A. S.; Vennard, T.; Fix, A.; Reimschuessel, R.; Overmann, G.; Shan, Y.; Daston, G. P. *Toxicol. Sci.* **2008**, 106, 251–262.
- (5) Lehn, J. M. *Supramolecular Chemistry*; VCH: Weinheim, Germany, 1995.
- (6) Fersht, A. R. *Trends Biochem. Sci.* **1987**, 12, 301–304.
- (7) Kitano, H.; Ringsdorf, H. *Bull. Chem. Soc. Jpn.* **1985**, 58, 2826–2828.
- (8) Leblanc, R. M. *Curr. Opin. Chem. Biol.* **2006**, 10, 529–536.
- (9) Ariga, K.; Kunitake, T. *Acc. Chem. Res.* **1998**, 31, 371–378.
- (10) Ariga, K.; Nakanishi, T.; Hill, J. P. *Soft Matter* **2006**, 2, 465–477.
- (11) Ahuja, R.; Caruso, P.-L.; Möbius, D.; Paulus, W.; Ringsdorf, H.; Wildburg, G. *Angew. Chem., Int. Ed.* **1993**, 32, 1033–1036.
- (12) Bohanon, T.; Denzinger, S.; Fink, R.; Paulus, W.; Ringsdorf, H.; Weck, M. *Angew. Chem., Int. Ed.* **1995**, 34, 58–60.
- (13) Weck, M.; Fink, R.; Ringsdorf, H. *Langmuir* **1997**, 13, 3515–3522.
- (14) Koyano, H.; Bissel, P.; Yoshihara, K.; Ariga, K.; Kunitake, T. *Langmuir* **1997**, 13, 5426–5432.
- (15) Koyano, H.; Bissel, P.; Yoshihara, K.; Ariga, K.; Kunitake, T. *Chem.–Eur. J.* **1997**, 3, 1077–1082.
- (16) Marchi-Artzner, V.; Artzner, F.; Karthaus, O.; Shimomura, M.; Ariga, K.; Kunitake, T.; Lehn, J.-M. *Langmuir* **1998**, 14, 5164–5171.
- (17) Huo, Q.; Dziri, L.; Desbat, B.; Russell, K. C.; Leblanc, R. M. *J. Phys. Chem. B* **1999**, 103, 2929–2934.
- (18) Hasegawa, T.; Hatada, Y.; Nishijo, J.; Umemura, J.; Huo, Q.; Leblanc, R. M. *J. Phys. Chem. B* **1999**, 103, 7505–7513.
- (19) Kovalchuk, N. M.; Vollhardt, D.; Fainerman, V. B.; Aksenenko, E. V. *J. Phys. Chem. B* **2007**, 111, 8283–8289.
- (20) Xu, W.; Wang, Y.; Xiao, Y.; Liu, F.; Lu, G.-Y. *Langmuir* **2009**, 25, 3646–3651.
- (21) Mendelsohn, R.; Braunder, J. W.; Gericke, A. *Annu. Rev. Phys. Chem.* **1995**, 46, 305–334.
- (22) Gericke, A.; Michailov, V.; Hühnerfuss, H. *Vib. Spectrosc.* **1993**, 4, 335–348.
- (23) Gericke, A.; Hühnerfuss, H. *J. Phys. Chem.* **1993**, 97, 12899–12908.
- (24) Flach, C. R.; Gericke, A.; Mendelsohn, R. *J. Phys. Chem. B* **1997**, 101, 58–65.
- (25) Gericke, A.; Flach, C. R.; Mendelsohn, R. *Biophys. J.* **1997**, 73, 492–499.
- (26) Bi, X.; Taneva, S.; Keough, K. M. W.; Mendelsohn, R.; Flach, C. R. *Biochemistry* **2001**, 40, 13659–13669.
- (27) Ren, Y.; Kato, T. *Langmuir* **2002**, 18, 6699–6705.
- (28) Du, X.; Miao, W.; Liang, Y. *J. Phys. Chem. B* **2005**, 109, 7428–7434.
- (29) Wang, Y.; Du, X.; Guo, L.; Liu, H. *J. Chem. Phys.* **2006**, 124, 134706.
- (30) Dyck, M.; Kerth, A.; Blume, A.; Lösche, M. *J. Phys. Chem. B* **2006**, 110, 22152–22159.
- (31) Zheng, J.; Leblanc, R. M. *Infrared Reflection Absorption Spectroscopy of Monolayers at the Air–Water Interface*. In *Advanced Chemistry of Monolayers at Interfaces*; Imae, T., Ed.; Elsevier B.V.: Amsterdam, 2007; Chapter 10.
- (32) Miao, W.; Du, X.; Liang, Y. *J. Phys. Chem. B* **2003**, 107, 13636–13642.

- (33) Wang, Y.; Du, X.; Miao, W.; Liang, Y. *J. Phys. Chem. B* **2006**, *110*, 4917–4923.
- (34) Smith, E. L. *J. Chem. Soc.* **1927**, 1288–1290.
- (35) Jeffrey, G. A.; Ghose, S.; Warwicker, J. O. *Acta Crystallogr.* **1961**, *14*, 881–887.
- (36) Wang, C.; Zheng, J.; Oliveira, O. N., Jr.; Leblanc, R. M. *J. Phys. Chem. C* **2007**, *111*, 7826–7833.
- (37) Liu, H.; Zheng, H.; Maio, W.; Du, X. *Langmuir* **2009**, *25*, 2941–2948.
- (38) Snyder, R. G. *J. Chem. Phys.* **1967**, *47*, 1316–1360.
- (39) Kawai, T.; Umemura, J.; Takenaka, T.; Kodama, N.; Seki, S. *J. Colloid Interface Sci.* **1985**, *103*, 56–61.
- (40) Barnes, A. J.; Le Gall, L.; Lauransan, J. *J. Mol. Struct.* **1979**, *56*, 15–27.
- (41) Snyder, R. G. *J. Mol. Spectrosc.* **1961**, *7*, 116–144.
- (42) Du, X.; Liang, Y. *J. Phys. Chem. B* **2004**, *108*, 5666–5670.
- (43) Andreeva, T. D.; Petrov, J. G.; Brezesinski, G.; Möhwald, H. *Langmuir* **2008**, *24*, 8001–8007.
- (44) Liao, K.; Du, X. *J. Phys. Chem. B* **2009**, *113*, 1396–1403.